

Induction of Melanoma in Murine Macrophage Inflammatory Protein 2 Transgenic Mice Heterozygous for Inhibitor of Kinase/Alternate Reading Frame¹

Jinming Yang,² Jing Luan,² Yingchun Yu,² Cunxi Li, Ronald A. DePinho, Lynda Chin, and Ann Richmond³

Veterans Affairs Medical Center and Department of Cancer Biology, Vanderbilt University School of Medicine Nashville, Tennessee 37232 [J. Y., J. L., Y. Y., C. L., A. R.], and Department of Adult Oncology, Dana-Farber Cancer Institute, Harvard Medical School, Boston, Massachusetts 02115 [R. A. D., L. C.]

ABSTRACT

The molecular and genetic events that contribute to the genesis and progression of cutaneous malignant melanoma are poorly understood, attributable in large part to the different genetic alterations accompanying tumorigenesis. Inhibitor of kinase 4a (INK4a) is often inactivated in families with hereditary melanoma. Loss of INK4a/alternate reading frame (ARF) in mice is associated with increased incidence of other tumors such as lymphoma and fibrosarcoma. However, the incidence of melanoma in INK4a/ARF-deficient mice is very low. Our previous studies have revealed that the CXC chemokine, CXCL1, is overexpressed in human malignant melanoma cells and is linked to transformation of immortalized murine melanocytes. To study the direct role of CXCL1 on the genesis of primary melanoma lesions, transgenic mouse lines were established that express the murine homologue of CXCL1, murine macrophage inflammatory protein 2 (MIP-2), under the transcriptional control of the tyrosinase promoter/enhancer (Tyr-MIP-2) in the mice that were deficient or not deficient for INK4a/ARF. Strong MIP-2 immunoreactivity was associated with pigmented melanocytes in the hyperproliferative hair follicles in the Tyr-MIP-2 transgenic mice, and the level of MIP-2 expression was similar in both INK4a/ARF heterozygous or wild-type mice. After treatment of mice with 7,12-dimethylbenz(a)anthracene, cutaneous melanomas formed in 12% (17/145) of the Tyr-MIP-2 transgene-positive mice, whereas only 2% (3/146) of the Tyr-MIP-2 transgene-negative mice developed melanoma. When melanocytes cultured from MIP-2 transgenic mice null for INK4a/ARF were transplanted into nude mice, melanoma formation occurred in 83% (10/12) of the cases with a latency period of 3 months. However, no melanoma lesions arose in nude mice injected with INK4a/ARF $-/-$ melanocytes, which did not express the MIP-2 transgene. Our results demonstrate that constitutive expression of MIP-2 in INK4a/ARF-deficient melanocytes facilitates formation of malignant melanoma.

INTRODUCTION

Because of the rapid rise in incidence, high metastatic propensity, and poor clinical prognosis of malignant melanoma, there is an urgent need to elucidate the genetic and molecular events involved in the etiology of this cancer (1, 2). Both environmental and genetic factors contribute to the origin and development of cutaneous melanoma (3–6). Genetic studies of atypical nevi and familial melanoma have led to the identification of several candidate melanoma loci within the human genome. The cytogenetic linkage for familial melanoma has been mapped to 9p21. The 9p21 locus contains the *INK4a*⁴ and *INK4b* genes that encode p16INK4a and p15INK4b, respectively (7). p16INK4a associates with the CDK4 (8) and inhibits the CDK4 and

CDK6 kinases (9), which are responsible for the phosphorylation of the RB. RB functions as a tumor suppressor protein, which negatively regulates passage of cells from G₁ into the S phase of the cell cycle by sequestering transcription factors such as E2F required for the G₁-S transition. Overexpression of p16INK4a inhibits the phosphorylation of RB by CDK4/cyclin D and facilitates cell cycle arrest in G₁ (10, 11). In addition to p16INK4a, the *INK4a* gene also encodes a growth inhibitor protein, termed p19^{ARF}, which initiates at an alternative 1st exon and shares exon 2 sequence with p16INK4a in alternative reading frame. p19ARF functions as negative regulator of cell cycle progression (12). p19ARF mediates cell cycle arrest or apoptosis through the p53 pathway (12) or directly interacts with other targets to inhibit cell proliferation (13, 14). The melanoma-specific mutations detected in 9p21 indicated that germ-line mutations exclusively targeted the *INK4a* gene (15). The *INK4b* gene exhibits physical proximity to the *INK4a* locus and encodes a p15 protein, which acts as an effector of transforming growth factor β -induced cell cycle arrest (16). In contrast to the cancer-prone phenotype of INK4a/ARF knockout mouse, which is doubly null for p16 and p19, the INK4b knockout did not reveal a potent cancer phenotype (17). However, whereas after more than two decades of effort a number of tumor suppressor genes have been associated with a predisposition to develop melanoma, only the *INK4a/ARF* locus has been genetically validated as a true melanoma susceptibility gene (15, 18). Moreover, in our study as well as in other reports, mice with INK4a/ARF knockout developed spontaneous tumors such as lymphoma and fibrosarcoma at an early age but few if any melanomas, even after treatment with DMBA or UV light (17). However, when expression of an activated *H-ras* gene was targeted to melanocytes using the tyrosinase promoter/enhancer, cutaneous melanoma lesions did develop (18). In addition to the *Ras* gene, a number of other oncogenes have been related to the genesis and progression of human melanoma, including *c-Met* (19), *SV-40* (20) and *GRO*, also known as MGSA or CXCL1.

The CXC chemokine *CXCL1/MGSA/GRO* is highly expressed in human Hs294T malignant melanoma cells. The MGSA protein was first purified and characterized in our laboratory (21, 22) and was subsequently found to have a sequence identical to the growth regulated gene, *GRO* (23). Since then, three genes encoding proteins with high homology to *MGSA* have been identified (*MGSA/GRO* α , β , and γ , now named as *CXCL1*, 2, and 3; Refs. 24, 25). *CXCL1* is overexpressed in viral, inflammatory, and neoplastic disease (26–29). Aberrant overexpression of *CXCL1* has been implicated in transformation and melanoma tumor progression both *in vivo* and *ex vivo* (30–32). During melanoma-malignant progression, both the *CXCL1* mRNA and protein levels are deregulated (33). Indeed, overexpression of *CXCL1* in immortalized melanocytes enables these cells to form tumors in nude and SCID mice, and antibodies to *CXCL1* suppress the growth of those tumors as well as reduce tumor angiogenesis (32). MIP-2, highly homologous to human MGSA, has been cloned and characterized (25). To explore the direct role of *CXCL1* on the genesis of melanoma, we created a transgenic mouse, which directed expression of MIP-2 to melanocytes through use of the tyrosinase promoter-enhancer elements to drive expression of *MIP-2* transgene. Transgenic MIP-2 founders were crossed with mice

Received 6/21/01; accepted 10/3/01.

The costs of publication of this article were defrayed in part by the payment of page charges. This article must therefore be hereby marked *advertisement* in accordance with 18 U.S.C. Section 1734 solely to indicate this fact.

¹ Supported by Department of Veterans Affairs Senior Career Scientist Award (to A. R.), NIH Grant CA56704 (to A. R.), and NIH Grant 5P30 AR41943.

² These authors made nearly equal contributions to this work.

³ To whom requests for reprints should be addressed, at Department of Cancer Biology, Vanderbilt University School of Medicine, Nashville, TN 37232. Phone: (615) 343-7777; Fax: (615) 343-4539; E-mail: Ann.Richmond@mcm.vanderbilt.edu.

⁴ The abbreviations used are: INK, inhibitor of kinase; MIP, murine macrophage inflammatory protein; RB, retinoblastoma protein; MGSA, melanoma growth stimulatory activity; GRO, growth regulated protein; ARF, alternate reading frame; DMBA, 7,12-dimethylbenz(a)anthracene; CDK, cyclin-dependent kinase.

(C57BL/6:129) deficient for the *INK4a/ARF* locus. MIP-2 transgenic mice on the *INK4a/ARF*-deficient background exhibited an increased incidence of cutaneous melanoma, increased size of papilloma lesions, and increased mortality after chemical induction with DMBA. Nude mice injected with melanocytes, which expressed the MIP-2 transgene but which were null for the tumor suppressor *INK4a/ARF* (*i.e.*, MIP-2⁺ and *INK4a/ARF*^{-/-}), formed melanoma tumor lesions. These data are compatible with a role for MIP-2 in melanoma tumor progression when tumor suppressor genes such as *INK4a/ARF* are deficient.

MATERIALS AND METHODS

MIP-2 Construct and Transgenic Model. The MIP-2 cDNA (1–430 bp; gift of Dr. Barbara Sherry, Picower Institute, New York, NY). This DNA was cloned into the *SmaI* site of the PIA plasmid that contained human β -globin intron and human growth hormone polyadenylation sequence. The tyrosinase promoter (2.5 kb of the 5-flanking sequences) and the newly identified distal enhancer element, 3.6 kb located 12 kb upstream of the promoter region (34), were placed in front of the human β -globin intron. A 7.7 kb *KpnI* fragment of DNA containing these sequence was excised, electrophoresed in a 1% low melting agarose gel, and purified by using Gel-ase enzyme. The human β -globin intron and human growth hormone polyadenylation sequence (gift of Dr. Manfred Blessing, University of Mainz, Mainz, Germany), and the tyrosinase promoter/enhancer (provided by Dr. Susan Porter, The University of British Columbia, Vancouver, British Columbia, Canada). The gel-purified 7.7 kb tyr-MIP-2 DNA construct was introduced into the pronuclei of C57BL/6 mice by pronuclear microinjection using standard protocols described (35). The MIP-2 transgene-positive F1 generation mice (either C57BL or BALB/c) was crossed with the *INK4a* knockout C57BL/6:129 mice established previously (35) to generate multiple founders. For MIP-2 and *INK4a* gene status, mouse tail DNA was analyzed by PCR using primers for MIP-2 (5' primer 5'-GGATGGCAACTTCCAGG-3', 3' primer 5'-TAATCCCAGCAATTTGGGAGGC-3'); 25 ng of tail DNA was amplified in the presence of 1.5 mM MgCl₂, 200 \times 4 μ M deoxynucleotide triphosphate mix, 1 unit of Taq polymerase (Life Technologies, Inc.), and 25 pmol of each primer in a final volume of 50 μ l. The PCR conditions were as follows: 94°C for 5 min followed by 94°C for 1 min, 57°C for 1 min 30 s, and 72°C for 2 min for 25 cycles with additional 72°C for 5 min after cycling. MIP-2-positive PCR products were 0.6 kb in size. The positive control for each PCR reaction used 25 pg of the Tyr-MIP-2 construct DNA. To confirm presence of the MIP-2 gene in transgenic mice, Southern blots or DNA dot blots were performed. Briefly, for dot blot, 10 μ g of DNA in 100 μ l of 10' SSC was loaded to the Genescreen membrane. For Southern blot, 10 μ g of DNA was digested with *NcoI* and *NotI*, fractionated on 1% agarose gel in Tris-Acetate-EDTA (TAE) buffer (0.04 M Tris-acetate, 0.001 M EDTA), then transferred to a Genescreen membrane. With this protocol, when the *NcoI* cut is made in the genomic DNA, the *NotI* site is preserved in the same manner in both the plasmid and the transgenic DNA, which has been integrated into the genomic DNA, such that the band detected by the radiolabeled human β -globin intron probe is the same size for both the plasmid and the genomic DNA. Dot blot and Southern blot were hybridized with ³²P-labeled human β -globin intron (0.6 kb *NcoI/SmaI* fragment from the PIA plasmid). The size of the MIP-2 transgene was 0.5 kb. For dot blot and Southern blot-positive control, 1 ng of DNA from the Tyr-MIP2 construct was used. As for identifying the *INK4a* genotype, three different primers (5'-TCCCTCTACTTTTCTTCTGAC-3'; 5'-CGGAACGCAAATATCGCAC-3'; and 5'-CTAGTGAGACGTGCTACTTC-3') were used in 50 μ l of PCR reaction (25 ng of tail DNA in the presence of 1.5 mM MgCl₂, 200 \times 4 μ M deoxynucleotide triphosphate mix, 1 unit of Taq polymerase and 25 pmol of each primer) programmed at 94°C for 5 min followed by 94°C for 1 min, 56°C for 1 min, and 72°C for 1 min for 35 cycles after an extension of 72°C for 5 min. DNA was separated on a 2% TAE-agarose gel. The banding pattern indicative of the *INK4a/ARF* null genotype was 313 bp; the *INK4a/ARF* wild type yielded a 278 bp band; the *INK4a/ARF* heterozygote yielded both PCR products (35).

DMBA Treatment of Mice and Tumor Development. Once MIP-2 transgenic founders were identified, the MIP-2 transgene-positive F₁ generation was crossed with C57BL/6:129 *INK4a/ARF*^{+/-} mice. The *INK4a/ARF*^{+/-},

MIP-2 transgene-positive mice from F-3 were crossed with *INK4a/ARF*^{+/-}, MIP-2 transgene-negative mice to generate MIP-2 transgene-positive or -negative mice on different *INK4a/ARF* genetic backgrounds (+/+, +/-, and -/-). Postnatal 5–8-week-old pups were treated with 100 μ l of 0.1% of DMBA (Sigma Chemical Co.) in acetone on bare back skin once a week for 5 weeks. Mice were shaved 1 week before the treatment. The occurrence of melanoma and papilloma was monitored by gross appearance and recorded weekly for each mouse. Tumor diameter was measured using calipers, and total tumor volumes were calculated based on these measurements. Primary skin tumors were adapted to culture by mechanical mincing with sterilized razor blades, trypsinization at 4°C for 6 h, dissociation into single cell suspension, followed by establishing cultures of viable cells in selective culture of 154 medium containing human melanocyte growth supplement (Cascade Biologicals, Inc.). These cells were passaged 8–15 generations in culture medium selective for melanocyte proliferation to reduce contamination by keratinocytes or fibroblasts from the original host. The purity of melanoma cells was carefully examined by microscopy. For the nude mouse explant experiments, 2 \times 10⁶ derivative melanoma cells were injected s.c. into the nude mice and observed for 14 days.

Isolation and Culture of Transgenic Melanocytes and Transplant in Nude Mice. Newborn pups from MIP-2 transgenic mice with an *INK4a/ARF*^{-/-} genotype were sacrificed by CO₂ asphyxiation. The mice were sterilized by soaking several times in Betadine Prep Solution and rinsed twice in ice-cold 70% ethanol. The skin was carefully peeled off, placed in HBSS with penicillin (100 units/ml), streptomycin (8.5 μ g/ml), and gentamicin (10 μ g/ml), then the peeled skin was placed dermis side down in a Petri dish containing blotting paper and 5 ml of 0.2% trypsin in HBSS containing penicillin (100 units/ml), streptomycin (8.5 μ g/ml), and gentamicin (10 μ g/ml); the Petri dish was placed in the refrigerator at 4°C overnight. The next day the trypsinized skins were carefully pulled away from the thin sheet of epidermis leaving the dermis on the blotting paper. The sheet of epidermis was rinsed in HBSS twice and cut in small pieces in 200 μ l of culture medium. The tissue pieces from one mouse were transferred into a 75-ml flask with 6 ml of 154 medium containing human melanocyte growth supplement (Cascade Biologicals, Inc.), and individual cells were released by pipetting up and down. After 3–4 days of culture, cells were treated with 0.25% trypsin/EDTA for 1–2 min to isolate melanocytes from keratinocytes. The cells were passaged 8–15 times in culture medium selective for melanocytes, and the purity of the cell population was evaluated by microscopy to verify the pigmentation of the cultures. For determination of expression of the transgene protein, the purified melanocytes from mice, which were MIP-2 transgene-positive or MIP-2 transgene-negative were plated in equal numbers into six-well plates in triplicate, cultured for 24 h, changed to serum-free medium, and cultured an additional 24 h. The medium was collected and analyzed for immunoreactive MIP-2 protein levels by the Quantikine ELISA kit (R & D) according to the manufacturer's procedures. The loss of the *INK4a/ARF* locus in these melanocytes was verified by PCR using DNA extracted from the cell cultures. Once the cultures of purified transgenic and nontransgenic melanocytes from *INK4a/ARF*^{-/-} mice were established *in vitro*, 2–8 \times 10⁶ cells of each genotype were injected into the subscapular region of nude mice.

MIP-2 Protein Analysis. Skin, kidney, and liver were collected from transgenic mice. Cytosolic proteins were extracted. Briefly the peeled pup skin was frozen in liquid nitrogen, the frozen skin was flashed with PBS, ground, and homogenized in 200 μ l of PBS. The homogenized tissue was centrifuged at 10,000 \times g for 15 min at 4°C to collect supernatant. MIP-2 levels were also determined in the skin of DMBA-treated C57BL/6 mice after two DMBA treatments using this procedure. Mouse blood was collected from mouse tails, allowed to clot at 4°C overnight, then blood samples were centrifuged, and serum was carefully separated. MIP-2 concentrations were measured using 200 mg of cytosolic proteins or serum following the standard protocol for the MIP-2 ELISA kit (R&D; Ref. 31).

Histological Analysis and Immunohistochemistry. Mice were euthanized, and tumor samples and their organs (lungs, liver, spleen, and kidneys) were collected and fixed in 4% paraformaldehyde in PBS (pH 7.6) for 24 h and postfixed in 70% ethanol. The fixed tissue was processed and embedded in paraffin using standard procedures. Tissue sections, which were 5- μ m thick, were cut and mounted on positively charged slides. H&E staining was performed according to standard protocols. For immunoperoxidase reaction, the Vectastain Elite ABC kit (# PK-7200; Vector Laboratories) was used. Briefly,

tissue sections were deparaffinized and rehydrated through xylenes and graded ethanol series, quenched for endogenous peroxidase activity by incubating the sections in 3% hydrogen peroxide in methanol, heated to enhance antigenicity, and blocked in diluted normal horse serum (# PK-7100) at room temperature for 30 min. Anti-S100 polyclonal antibody (1:600 dilution; #Z0628; Dako Corporation), rabbit polyclonal antiserum against MIP-2 (1:100 dilution; a gift from Bob Streiter, University of California Los Angeles, Los Angeles, CA), rabbit polyclonal antibody against p16INK4a (1:50 dilution; a gift from Charles J. Sherr, St. Jude Children's Research Hospital, Memphis, TN), and rabbit polyclonal antibody against p53 (1:50 dilution; FL-393; Santa Cruz Biotechnology) were diluted in blocking solution, incubated on tissue sections at room temperature for 1 h or at 4°C for overnight, and washed in PBS. Sections were subsequently incubated with secondary biotinylated antibody (# PK-7100) and avidin-biotin peroxidase complexes (# PK-7100) following the standard protocol. AEC substrate (# K3469) was used as the chromogen, and hematoxylin was used as the nuclear counterstain. Positive staining appears as a red color on a blue nuclear background of cells.

RESULTS

Transgenic MIP-2 Model and Gene Expression. Maximal expression of melanocyte-specific transgenes has been obtained using 2.5 kb of 5'-flanking sequences along with the melanocyte-specific enhancer of a 3.6 kb of 5' flanking sequence of the mouse tyrosinase gene promoter (34). We used this 6.1-kb tyrosinase promoter/enhancer to direct expression of the MIP-2 transgene (Fig. 1A). Together these promoter/enhancer regions confer enhanced and copy number-related expression in melanocytes. Transgenic MIP-2 founders were confirmed by PCR, Southern blot, and dot blot (Fig. 1B). Four sets of newborn founders appeared morphologically and phenotypically normal. One founder line exhibited short tails and short limbs, attributable to the site of integration of the transgene. Founders, which were phenotypically normal, possessed high transgenic copy number, and transmitted the MIP-2 transgene to their offspring, were crossed with *INK4a/ARF*^{-/-} mice characterized previously (18) to create the mixed genetic background. Progeny were developed having six genetic backgrounds (*INK4a/ARF*^{+/+}; *INK4a/ARF*^{+/-}; and *INK4a/ARF*^{-/-}) for both transgenic MIP-2 and nontransgenic mice.

To examine whether the MIP-2 transgene was expressed in potential founders, the total cellular RNA samples derived from both transgenic and nontransgenic adult mouse skin were assayed by Northern blot analysis for specific hybridization to α -³²P-labeled human growth hormone polyadenylation fragment from the MIP-2 expression vector. The results in Fig. 1C show that a strong hybridization signal was obtained from transgenic skin RNA samples (Fig. 1C, Lane 4) but was barely observed in nontransgenic skin (Fig. 1C, Lane 3) under equal total RNA loading (Fig. 1C, Lanes 1 and 2). The identical outcome was obtained when the Northern blot was probed with ³²P-labeled MIP-2 cDNA (data not shown). To determine whether this enhanced MIP-2 mRNA correlated with enhanced MIP-2 protein expression in transgenic mice, MIP-2 concentrations in serum and cytosolic extracts from skin of both transgenic and nontransgenic mice were assayed by ELISA. As expected, MIP-2 protein was highly expressed in transgenic skin (3610 ± 500 pg/mg protein) as compared with the nontransgenic skin (150 ± 100 pg/mg protein). Similarly, serum MIP-2 protein levels were obviously higher in MIP-2 transgenic mice (2142 ± 380 pg/mg protein) than in nontransgenic mice (86 ± 80 pg/mg protein). Loss of *INK4a/ARF* did not affect the production or secretion of MIP-2. The MIP-2 protein levels from Tyr-MIP-2 transgenic mice with different *INK4a/ARF* ($+/+$, $+/-$, and $-/-$) genetic backgrounds were very similar, based on Northern data, ELISA data from serum samples, as well as MIP-2 immunostaining of skin sections (data not shown). The data in Fig. 1D indicate

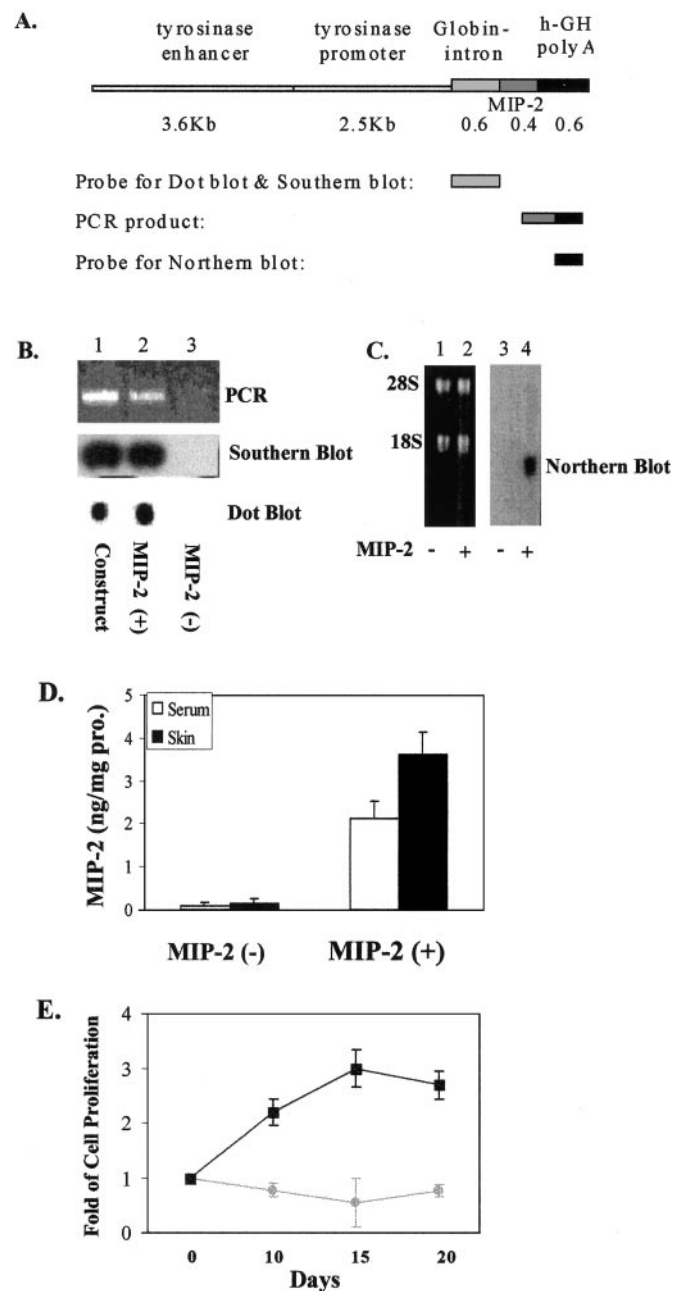


Fig. 1. Tyr-MIP-2 construct and gene expression. A, schematic construct of Tyr-MIP-2 transgene; B, murine MIP-2 transgene was identified with DNA extracted from mouse tail by PCR, Southern blot, and dot blot; C, Northern blot verification of expression of the MIP-2 transgene mRNA in skin of transgenic mice; D, ELISA analysis of MIP-2 protein expression levels in serum and skin tissue of transgenic mice; and E, cell growth was observed by *in vitro* cultured *INK4a/ARF* knockout melanocytes, which expressed the MIP-2 transgene (■) or were nontransgenic (●) in serum-free 154 medium for the indicated days. Data shown are representative of triplicate experiments; bars, \pm SD.

that there is an \sim 24-fold increase in MIP-2 protein expression in transgenic mice as compared with the nontransgenic mice. However, this was not associated with any obvious phenotype in an unstressed animal. The transgenic mice were of normal size, mated normally, had similar sized litters, similar coat color, and a similar life expectancy as the nontransgenic mice. To determine whether overexpression of the MIP-2 oncoprotein confers a melanocyte growth advantage, the melanocytes derived from *INK4a/ARF* null mice that expressed or did not express MIP-2 transgene were cultured at a density of 10^4 cells/ml in a six-well plate in serum-free medium for different days, and the cell number was counted. As indicated in Fig. 1E, Tyr-MIP-2 + *INK4a/*

ARF $-/-$ cells increased in cell number 2–3-fold over a time period of 10 and 15 days, in contrast to Tyr-MIP-2-INK4a/ARF $-/-$ cells, which failed to proliferate under the same serum-free culture conditions. This is the same level of induction that addition of exogenous MIP-2 to normal melanocyte cultures produces (33), so it is likely that loss of INK4a/ARF is related to immortalization, but expression of MIP-2 is related to proliferative advantage of melanocytes.

Incidence of Cutaneous Melanoma in MIP-2 Transgenic Mice.

Because genetic background can affect the tendency to form specific types of tumors, we choose to develop MIP-2 transgenic mice on two different genetic backgrounds: C57BL/6 and BALB/c. Although BALB/c mice are albino, they still have melanocytes, which are capable of expressing the Tyr/MIP-2 transgene and forming amelanotic tumors. The defect in these mice has to do with production of melanin attributable to defective production of tyrosinase. These BALB/c mice carrying the MIP-2 transgene were crossed with the INK4a/ARF heterozygous mice on a C57BL/6/129 background to produce mice carrying the MIP-2 transgene on a black background as well as on a white background. We expanded the mice generated from this founder with the black background carrying the MIP-2 transgene for this study. The melanoma tumors formed on this Tyr-MIP-2/INK4a $+/-$ background after DMBA treatment were pigmented, as would be expected, because the mice were pigmented. Once MIP-2 transgenic mice were established on the C57BL/6/129 mice of different INK4a/ARF genetic backgrounds ($+/+$, $+/-$, $-/-$), a total of 500 μ g of DMBA was topically administered to 5–8-week-old pups over 5 weeks. DMBA treatment itself induced MIP-2 expression in the skin of treated mice to a level comparable with that of the MIP-2 transgenic mice (\sim 26 fold induction compared with untreated wild-type mice), though this induction would be transient and not be sustained as it was in the transgenic mice.

Observations were made on the DMBA-treated mice through week 40. However, the majority of mice null for INK4a/ARF died early in the course of the experiment (12–17 weeks) because of rapidly progressing lymphoma, too soon to observe the MIP-2 transgene influence on the genesis of melanoma. This occurred even without DMBA treatment in the INK4a/ARF $-/-$ mice. The cohort studies here were based on breeding INK4a/ARF $+/-$ mice with either of two founders of MIP-2 transgenic animals, one on the C57BL background and the other on the BALB/c background. The results summarized in Tables 1 and 2 and Figs. 2 and 3 represent data from experiments performed on progeny from two MIP-2 transgenic founders. Two types of controls were used: (a) the nontransgenic mice were treated following the same protocols as for transgenic animal; and (b) the solvent acetone was used to treat transgenic and nontransgenic mice as a negative control. The results show that 17 cases of cutaneous melanoma arose from 145 transgenic mice in which 44% mice had wild-

Table 1 Tumor development after DMBA treatment of mice

Transgenic mice were topically treated with 100 μ g DMBA once a week for 5 weeks. Non-transgenic mice were treated with the same protocol as a control group. With the similar cohort size and INK4a/ARF background, melanoma tumor formation was significantly higher in the MIP-2 transgene positive group than in the MIP-2 negative group ($P < 0.01$, Chi Square Test). The development of other tumors (including liver carcinoma, fibrosarcoma and lymphoma) and the mean volume of papillomas was increased in MIP-2 transgenic mice as compared to non-transgenic mice of the same INK4a/ARF genotype.

MIP-2 transgene	Cohort size	INK4a/ARF Genotype distribution	Melanomas				Other tumors	Papilloma size (mm)
			n	Incidence	Latency			
Negative	146	$+/+$ 38% (55/146)	3	2%	190 \pm 82d	3	1.25 \pm 1.1	
		$+/-$ 62% (91/146)						
		$-/-$ 0%						
Positive	145	$+/+$ 44% (64/145)	17	12% ^a	195 \pm 42d	14 ^a	2.85 \pm 2.1 ^a	
		$+/-$ 56% (81/145)						
		$-/-$ 0%						

^a $P < 0.01$.

Table 2 Genotype analysis of melanomas that arose from transgenic mice

Melanoma tumor formation associated with INK4a/ARF deficiency was analyzed by the case-control method. Among 20 melanoma cases, 18 melanomas were deficient for INK4a/ARF but only 2 cases occurred in the INK4a/ARF wild type group. These data suggest that inactivation of INK4a/ARF significantly contributed to MIP-2-induced murine skin melanoma formation ($P < 0.01$, by Chi-Square Test).

Genotype	MIP-2 transgene negative		MIP-2 transgene positive	
	n	Melanoma incidence	n	Melanoma incidence
INK4a/ARF				
$+/+$	0	0% (0/55)	2	3.1% (2/64)
$+/-$	3	3.3% (3/91)	15 ^a	18.5% (15/81)

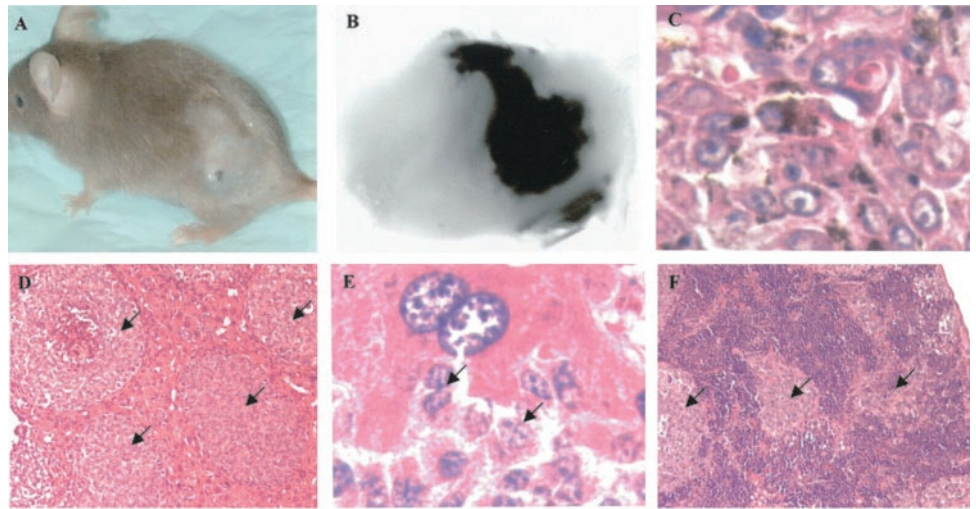
^a $P < 0.01$.

type INK4a/ARF and 56% mice had heterozygous INK4a/ARF background. The latency period was 195 \pm 42 days. Only 3 cases of cutaneous melanoma developed from 146 nontransgenic animals, of which the INK4a/ARF background was wild type in 38% of the mice and heterozygous in 62% of the mice. The data shown in Table 1 demonstrate that after DMBA treatment, the MIP-2 transgenic mice exhibited a significant increase in the incidence of melanoma (12%; $P < 0.01$) as compared with the nontransgenic group (2%) with similar INK4a/ARF genetic background (INK4a/ARF $+/+$ and INK4a/ARF $+/-$). Mice treated with acetone alone did not exhibit any skin lesions of melanoma or papilloma. Table 2 summarizes the comparative analysis of INK4a/ARF genotype in the cutaneous melanoma lesions, which developed from transgenic mice. There were 20 mice that developed primary melanoma of a total population of 291 mice, the genotypes of which were MIP-2+/INK4a/ARF $+/-$; MIP-2+/INK4a/ARF $+/+$; MIP-2-/INK4a/ARF $+/-$; and MIP-2-/INK4a/ARF $+/+$. No melanoma lesions (0%) appeared in 55 MIP-2-/INK4a $+/+$ mice; 2 cases of melanoma were observed in 64 MIP-2+/INK4a $+/+$ mice (3.1%), 3 melanoma lesions were observed in 91 MIP-2-/INK4a $+/-$ mice (3.3%), and 15 melanoma lesions formed in 81 MIP-2+/INK4a $+/-$ mice (18.5%; $P < 0.01$). Our results support the hypothesis that INK4a/ARF heterozygosity increases the likelihood of development of melanoma after carcinogen treatment. In these experiments, mice bearing melanoma lesions were sacrificed before the tumors became invasive, and we did not observe metastasis under these experimental conditions. In addition, we observed that MIP-2 transgenic mice also developed lymphoma, fibrosarcoma, and hepatocellular carcinoma related to INK4a/ARF $+/-$ background (Table 1). After DMBA treatment, papilloma lesions developed in both MIP-2 transgenic and nontransgenic mice with or without expression of both INK4a/ARF alleles. The size of papilloma lesions, which developed in the MIP-2 transgenic mice (2.8 \pm 2.1 mm), was larger than that in nontransgenic group (1.25 \pm 1.1 mm; $P < 0.01$). These lesions tended to merge over time, so we were unable to determine whether there were differences in the number of papilloma lesions. The survival time after DMBA treatment was decreased in MIP-2 transgenic mice ($P < 0.05$) as compared with the nontransgenic animals on the same genetic background (data not shown).

To evaluate the potent tumorigenicity and metastatic capacity of primary cutaneous melanomas from MIP-2 transgenic mice, cells were isolated from these tumor lesions, cultured *in vitro*, and injected into nude mice, and the animals were observed for tumor formation. Melanomas formed in the mice injected s.c. with 4×10^5 cells within 2 weeks. The tumors were invasive to adjacent muscle, and in some mice, metastasis to liver (Fig. 2, D and E) and lymph node (Fig. 2F) were observed.

Immunohistochemistry and Histological Analysis. S-100 is a marker for neural crest-derived cells often used diagnostically for melanoma lesions. We characterized the S-100 immunoreactivity in

Fig. 2. Histological analysis of melanoma and metastasis. *A*, typical cutaneous pigmented melanoma lesion arising in MIP-2 transgenic mice heterozygous for INK4a/ARF; *B*, morphology of the melanoma; and *C*, H&E staining of tissue section from a typical pigmented melanoma arising in MIP-2 transgenic mice. Melanoma cultures established from primary melanoma were injected into the subscapular region of nude mice. *D*, the melanoma cells formed a tumor, which metastasized to liver, $\times 10$ magnification and $\times 50$ magnification (*E*), and to lymph node (*F*) $\times 10$ magnification. Arrow, melanoma lesions.



skin tumor lesions arising in these transgenic mice (Fig. 3A) and found that S-100 immunoreactive protein is expressed frequently in the dermal lesions of melanoma. Some pigmented cells exhibited atypic nuclei. No S-100 immunoreactivity was observed when primary antibody was substituted with normal serum or omitted from the immunostaining procedures (data not shown). Together with S-100 staining (Fig. 2, *B* and *C*, and Fig. 3B) and histological analysis of these lesions by a clinical pathologist (Dr. David Page, Vanderbilt University), the diagnosis of melanoma was confirmed. To examine the distribution of MIP-2 protein in the skin lesions, MIP-2 immunostaining was performed on C57BL/6 and BALB/c mice expressing and not expressing the MIP-2 transgene, and in mice INK4a/ARF+/+ and +/- . Pigmented melanoma lesions arising in MIP-2 transgenic mice exhibited fairly strong MIP-2 immunoreactivity, and even stron-

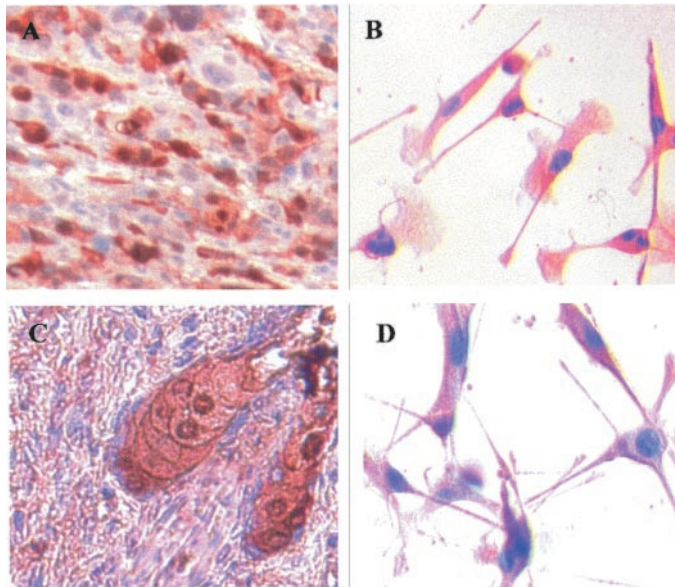


Fig. 3. Immunohistochemistry of sections from primary melanoma or derived culture cells. Tissue from cutaneous melanoma lesion that developed on MIP-2 transgenic mice were fixed, embedded, and immunostained for S-100 protein using the anti-S-100 polyclonal antibody (# Z0628; Dako Corporation). *A*, $\times 50$ magnification, and (*B*) culture cells derived from the melanoma lesion were also immunoreactive for S-100 (*A*). Sections from MIP-2-positive melanoma tumors were immunostained with anti-MIP-2 polyclonal antibody (*C*), $\times 50$ magnification showed a strong immunoreactivity in the base of hair follicle coincident with pigmented cells, and (*D*) cultured cells derived from primary melanoma from MIP-2 transgenic-positive and INK4a/ARF+/- mice were also immunoreactive for MIP-2 polyclonal antibody.

Table 3 Melanoma formation in the nude mice transplanted with melanocytes null for INK4a/ARF

The epidermal melanocytes derived from either MIP-2 transgenic or non-transgenic new born mice null for p16 INK4a/ARF were inoculated into the subscapular region of nude mice. After approximately 3 to 4 months of latency, melanomas only formed in the nude mice injected with MIP-2 transgene positive melanocytes but not in mice injected with of INK4a/ARF-/- melanocytes which do not express the MIP-2 transgene. Values in the table are pooled data from two independent experiments.

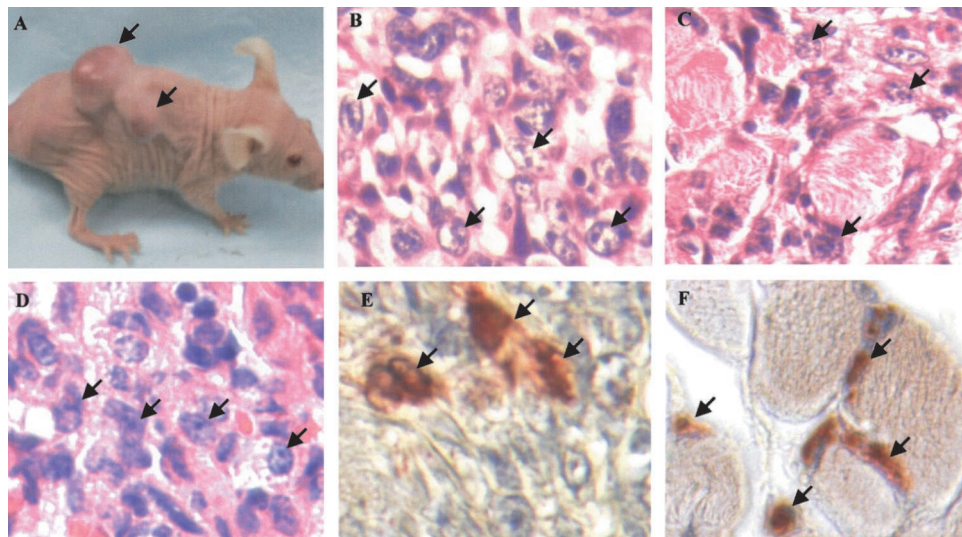
Genotype of melanocytes		Melanomas				
MIP-2 transgene	INK4a/ARF status	Cohort size	<i>n</i>	Incidence	Latency	Metastatic tumors
-	-/-	14	0	0%		0
+	-/-	12	10	83% ^a	93 ± 48d	4

^a $P < 0.01$.

ger immunoreactivity was associated with pigmented melanocytes in the hyperproliferative hair follicles (Fig. 3C). These data are in agreement with the ELISA results from transgenic mouse skin. A weak MIP-2 immunoreactivity was also observed in kidney, liver, and lung tissues (data not shown), and this occurs in transgenic and nontransgenic mice and is not related to the INK4a/ARF status. To explore the possibilities of loss of the tumor suppressor protein p16INK4a or mutation of the p53 protein in the melanoma tumors that formed, immunostaining for p16INK4a or mutant p53 were performed on the identified murine melanomas and their cultured cells derived from these tumor lesions. These cutaneous melanomas, either INK4a/ARF wild type or heterozygous, did not stain with antibody for the mutant p53 (data not shown), suggesting that p53 was not mutated in the melanocytes that formed tumors. PCR analysis of the DNA from cultures established from the melanoma tumors that arose on mice with the INK4a/ARF+/- background were heterozygous for INK4a/ARF (data not shown). p16INK4a immunostaining using an antibody from Charles Sherr, which does not recognize p15 or p19 revealed that there was heterogeneity within the tumors in regard to nuclear localization of p16INK4a. These data suggest that loss of p16INK4a may selectively occur in some of the melanoma cells in tumors, which develop on the MIP-2 transgene-positive INK4a/ARF heterozygous background in some but not all instances. However, it is difficult to be absolutely sure that the cells staining positively for INK4a within the tumor are indeed tumor cells as compared with stromal cells brought into the rapidly growing tumor.

Melanoma Formation in Nude Mice Transplanted with MIP-2 Transgenic Melanocytes Null for INK4a/ARF. Overexpression of MIP-2 in melanocytes was associated with an increase in the inci-

Fig. 4. Melanoma formation in nude mice transplanted with MIP-2-transgenic melanocytes that were null for INK4a/ARF. Two million epidermal melanocytes derived from MIP-2-transgenic newborn mouse completely deficient for INK4a/ARF were injected in the subscapular region of nude mice. A, after 101 days of latency, skin melanoma lesions were observed; B, H&E staining reveals the histological characteristics of a melanocytic tumor lesion; C, melanoma cells were observed invading the underlying muscle; D, melanoma tumor cells also metastasize to the lung; E, S-100 immunostaining of tumor cells in lung; and F, S-100 immunostaining of tumor cells invading muscle. Arrow indicates melanoma lesions or typical melanoma cells.



dence of cutaneous melanoma in C57BL/6 mice induced with DMBA. To additionally explore the possibility that MIP-2 expression could directly induce melanocyte transformation without addition of a chemical carcinogen, we isolated melanocytes from two newborn pups of MIP-2 transgenic or nontransgenic mice null for INK4a/ARF and amplified them *in vitro*. Subsequently, two independent experiments were performed where different numbers of cells were inoculated into the subscapular region of nude mice. Both experiments showed similar results, and the data are summarized in Table 3. Melanoma tumors were observed at the site of inoculation with Tyr-MIP-2 transgene-positive melanocytes null for INK4a/ARF (Fig. 4A) with significant blood vessels formation on tumor surface after 3–4 months of latency. In the first experiment, four nude mice were inoculated with 8.4×10^6 INK4a/ARF^{-/-} Tyr-MIP-2 transgene-positive cells/animal, and all four of the mice developed melanoma. A second group of eight nude mice were inoculated with 2×10^6 INK4a/ARF^{-/-} Tyr-MIP-2 transgene-positive cells/mouse, and six of the eight mice developed melanoma. In contrast, no melanoma tumors appeared on those nude mice inoculated with the same number of melanocytes cultured from nontransgenic INK4a/ARF null mice (Tyr-MIP-2⁻, INK4a/ARF^{-/-}), even when the observation time was extended for 2 additional months. The histological characteristics of cutaneous pigmented lesions were typical for melanoma (Fig. 4B). The transformed melanocytes showed the capacity for metastasis to lung (Fig. 4, D and E) and invasion into muscle adjacent to the tumor (Fig. 4, C and F). Apart from histological analysis, S-100 was examined to confirm the neural crest origin of the tumor cells (Fig. 4, E and F). Moreover, the presence of pigment in the cell cultures established from these tumor lesions additionally confirmed the melanocytic origin of the tumor (data not shown).

DISCUSSION

In this study, we have shown for the first time that overexpression of MIP-2 in melanocytes increased the formation of DMBA-induced melanoma lesions in mice that were heterozygous for INK4a/ARF. To obtain more insight into the causal relationship between MIP-2 gene expression and melanoma formation, nude mice were transplanted with MIP-2-positive melanocytes completely deficient in INK4a/ARF. Results show that melanoma tumors formed with a relatively short latency, whereas no tumors formed when INK4a/ARF^{-/-} melanocytes not expressing the MIP-2 transgene were injected into

the mice. These data provide a molecular link between constitutive expression of MIP-2 in melanocytes and transformation.

Although the INK4a/ARF tumor suppressor gene has been shown to be mutated in melanoma-prone families, the lower frequency of loss of INK4a/ARF in spontaneous melanoma lesions, coupled with the linkage of loss of this gene with numerous other cancers (36), led some investigators to question the role of INK4a/ARF as the melanoma gene. Moreover, mice deficient in INK4a/ARF did not develop melanoma lesions unless a second factor such as oncogene *H-ras* was overexpressed in melanocytes (18). More recently, “pure” INK4a/p16 null mice have been developed, and the incidence of spontaneous tumor formation in these mice was evaluated (37, 38). In one study the spontaneous tumor incidence was low and not statistically significant as compared with wild-type mice (37), whereas another study showed that loss of p16INK4a resulted in enhanced tumor formation, reduced tumor-free survival with a low incidence of spontaneous and carcinogen-induced melanoma, and reduced tumor-free survival after DMBA treatment (38). Moreover, fibroblasts cultured from these mice grew and underwent senescence similar to those from wild-type mice (37, 38). However, when mice homozygous for the loss of p16INK4a and heterozygous for the loss of p19/ARF (INK4a^{*Δ} 2,3) were developed, a wide variety of tumors formed including sarcomas, carcinomas, lymphoma, and melanoma (37). A single dose of DMBA treatment for INK4a^{*Δ} 2,3 mice resulted in 50% incidence of cutaneous melanoma between 3 and 9 months of age, and 3 of 8 melanoma lesions showed metastasis to lymph nodes, lungs, spleen, or liver (37).

In our study, a 24-fold-increased expression of the MIP-2 transgene in melanocytes was accompanied by a 6-fold-increased incidence of skin melanoma in mice, which were heterozygous for INK4a/ARF^{+/-}. Melanocytes completely deficient for INK4a/ARF, which did not express the MIP-2 transgene, did not form melanoma lesions in nude mice, whereas 83% of the mice injected with MIP-2 transgene-expressing INK4a/ARF^{-/-} melanocytes formed melanoma lesions. We reasoned that the deficient INK4a/ARF may serve as a melanoma susceptibility modifier, which requires cooperation with an activated oncogene for tumor formation to occur. The selection of MIP-2 as the cooperating oncogene in our model was based on our previous findings that MGSA, the human homologue for MIP-2, was overexpressed in human malignant melanoma and was associated with enhanced ras activity and constitutive IκB kinase-nuclear fac-

tor- κ B signaling. Both of these later events support maintenance of the malignant state (28, 39). Moreover, overexpression of MGSA in immortalized melanocytes induces transformation (24, 31) and promotes angiogenesis on the course of tumorigenesis (40). Taken together with previous observations (22, 39), this study demonstrates that MIP-2 can play an important role in transformation of melanocytes, which exhibit an underlying INK4a/ARF deficiency. However, it should be noted that we did not observe spontaneous melanoma lesions in the MIP-2+/INK4a/ARF+/- and in the MIP-2+/INK4a/ARF-/- mice. The mice are overtaken with lymphoma too early to allow sufficient time for development of melanoma. With carcinogen treatment, the incidence of melanoma development in the INK4a/ARF+/- mice is 12%, suggesting that retention of one INK4a/ARF allele is protective, even in the face of overexpression of MIP-2. This conclusion is compatible with the recent findings with the DMBA-treated INK4a^{* Δ} 2,3 mice (37). We observed that DMBA treatment itself can markedly induce the expression of MIP-2 (data not shown). This induction of MIP-2 by DMBA may facilitate papilloma formation but not melanoma formation, because only in the Tyr-MIP-2-transgenic mice exhibiting continuous expression of MIP-2 in melanocytes under the direction of the tyrosinase promoter/enhancer did we observe enhanced melanoma tumor formation after DMBA treatment. Moreover, the DMBA induction of melanoma occurred only in the mice with an INK4a/ARF+/- genetic background.

A role for INK4a/ARF as a potent tumor suppressor gene has been clearly established (35). In this study, analysis of the INK4a/ARF genotype in melanoma lesions revealed that 90% (18/20) of melanomas were deficient for one of the INK4a/ARF alleles (Table 2). p16INK4a, as an inhibitor of CDK, negatively regulates cell cycle. p19ARF triggers the p53-dependent checkpoint. Loss of either of these tumor suppressors may be associated with tumor formation (9, 12). In our experiments in nude mice loss of INK4a/ARF alone was not sufficient to induce melanoma. However, loss of INK4a/ARF coupled with MIP-2 transgene expression in melanocytes results in melanoma tumor formation in the nude mouse xenograft model. On the basis of these observations, we suggest that enhanced MIP-2 expression in cooperation with loss of INK4a/ARF may play a potent role in the induction of melanoma *in vivo*. Whereas in the experiments described here we did not attempt to inject MIP-2 transgene-expressing melanocytes of an INK4a/ARF+/+ background into nude mice to determine whether tumors form, it is intuitive that because there is no *in vitro* immortalization or transformation event in the absence of loss of one of the INK4a/ARF alleles, tumors would not form. Moreover, melanocyte cell cultures established from MIP-2 transgene-positive INK4a/ARF+/+ mice could not be continuously passaged and expanded sufficiently to provide the numbers of cells required for the experiment.

The development of tumorigenicity, invasion, and metastasis in nude mice after injection of cultured cells derived from primary melanoma lesions, which arose in MIP-2 transgene-positive INK4a/ARF+/- mice, indicates that MIP-2 expression facilitates metastatic potential. However, the mechanistic link between MIP-2 pathways and melanoma metastasis is not well characterized. 12-*O*-tetradecanoylphorbol-13-acetate induction of MIP-2 expression in mice is associated with enhanced neutrophil infiltration, keratinocyte proliferation, and papilloma formation after DMBA treatment (41). MIP-2 has also been reported to recruit natural killer T cells to the spleen during tolerance induction, so enhanced production of MIP-2 might play some role in facilitating peripheral tolerance to the developing tumor (42). Expression of CXCL8 in human melanoma lesions correlates with enhanced metastatic capacity (43, 44). In the DMBA-induced melanoma lesions, which arose on the mice heterozygous for INK4a/ARF, mice had to be sacrificed before the mice were overtaken

with lymphoma or fibrosarcoma, so we could not follow these lesions for sufficient time to determine whether metastasis might occur if the tumors grew larger. In the transgenic model described here, MIP-2, plays a role in the genesis of primary skin melanoma, and INK4a/ARF deficiency may play a synergistic role with MIP-2 gene in melanocyte transformation. A role for MIP-2 in melanoma metastasis cannot be ruled out.

ACKNOWLEDGMENTS

We thank David Page (Vanderbilt University School of Medicine, Nashville, TN) for critically reading the pathology of slide/tissue sections of mouse skin tumor; Barbara Sherry (Picower Institute, New York, NY) for the MIP-2 cDNA; Susan Porter for tyrosinase enhancer and promoter; Manfred Blessing (University of Mainz, Mainz, Germany) for the human β -globin intron and growth hormone polyadenylation sequence; Robert Strieter (UCLA, Los Angeles, CA) for the antibody to murine MIP-2; Charles Sherr (St. Jude's Hospital, Memphis, TN) for the antibody to murine p16INK4a; Matt Devalaraja for assistance in delivery of DMBA to mice; and Ben Johnson and Linda W. Horton (Vanderbilt University, Nashville, TN) for technical assistance.

REFERENCES

- Rigel, D. S., Friedman, R. J., and Kopf, A. W. Lifetime risk for development of skin cancer in the U. S. population: current estimate is now 1 in 5. *J. Am. Acad. Dermatol.*, 35: 1012-1013, 1996.
- Herlyn, M., Hoska, S., Akahoshi, T., Wada, C., and Kondo, H. Expression of the chemokine superfamily in rheumatoid arthritis. *Clin. Exp. Immunol.*, 97: 451-457, 1994.
- Tormanen, V. T., and Pfeifer, G. P. Mapping of UV photoproducts within ras proto-oncogenes in UV-irradiated cells: correlation with mutations in human skin cancer. *Oncogene*, 7: 1729-1736, 1992.
- Tornaletti, S., Rozek, D., and Pfeifer, G. P. The distribution of UV photoproducts along the human p53 gene and its relation to mutations in skin cancer. *Oncogene*, 8: 2051-2057, 1993.
- Pollock, P. M., Yu, F., Qiu, L., Parsons, P. G., and Hayward, N. K. Evidence for u.v. induction of CDKN2 mutations in melanoma cell lines. *Oncogene*, 11: 663-668, 1995.
- Jiveskog, S., Ragnarsson-Olding, B., Platz, A., and Ringborg, U. N-ras mutations are common in melanomas from sun-exposed skin of humans but rare in mucosal membranes or unexposed skin. *J. Invest. Dermatol.*, 111: 757-761, 1998.
- Kamb, A., Gruis, N. A., Weaver-Feldhaus, J., Liu, Q., Harshman, K., Tavtigian, S. V., Stockert, E., Day, R. S., III, Johnson, B. E., and Skolnick, M. H. A cell cycle regulator potentially involved in genesis of many tumor types. *Science (Wash. DC)*, 264: 436-440, 1994.
- Xiong, Y., Zhang, H., and Beach, D. Subunit rearrangement of the cyclin-dependent kinases is associated with cellular transformation. *Genes Dev.*, 7: 1572-1583, 1993.
- Sherr, C. J., and Roberts, J. M. CDK inhibitors: positive and negative regulators of G1-phase progression. *Genes Dev.*, 13: 1501-1512, 1999.
- Serrano, M., Gomez-Lahoz, E., DePinho, R. A., Beach, D., and Bar-Sagi, D. Inhibition of ras-induced proliferation and cellular transformation by p16INK4. *Science (Wash. DC)*, 267: 249-252, 1995.
- Lukas, J., Parry, D., Aagaard, L., Mann, D. J., Bartkova, J., Strauss, M., Peters, G., and Bartek, J. Retinoblastoma-protein-dependent cell-cycle inhibition by the tumour suppressor p16. *Nature (Lond.)*, 375: 503-506, 1995.
- Sherr, C. J. Tumor surveillance via the ARF-p53 pathway. *Genes Dev.*, 12: 2984-2991, 1998.
- Pomerantz, J., Schreiber-Agus, N., Liegeois, N. J., Silverman, A., Alland, L., Chin, L., Potes, J., Chen, K., Orlow, I., Lee, H. W., Cordon-Cardo, C., and DePinho, R. A. The INK4a/ARF tumor suppressor gene product, p19Arf, interacts with MDM2 and neutralizes MDM2's inhibition of p53. *Cell*, 92: 713-723, 1998.
- Sharpless, N. E., and DePinho, R. A. The INK4a/ARF locus and its two gene products. *Curr. Opin. Genet. Dev.*, 9: 22-30, 1999.
- Hussussian, C. J., Struwing, J. P., Goldstein, A. M., Higgins, P. A., Ally, D. S., Sheahan, M. D., Clark, W. H., Jr., Tucker, M. A., and Dracopoli, N. C. Germline p16 mutations in familial melanoma. *Nat. Genet.*, 8: 15-21, 1994.
- Hannon, G. J., and Beach, D. p15INK4B is a potential effector of TGF- β -induced cell cycle arrest. *Nature (Lond.)*, 371: 257-261, 1994.
- Serrano, M. A., Lee, H., Chin, L., Cordon-Cardo, C., Beach, D., and DePinho, R. A. Role of the INK4a locus in tumor suppression and cell mortality. *Cell*, 85: 27-37, 1996.
- Chin, L., Pomerantz, J., Polsky, D., Jacobson, M., Cohen, C., Cordon-Cardo, C., Horner, J. W., Jr., and DePinho, R. A. Cooperative effects of INK4a/ARF and ras in melanoma susceptibility *in vivo*. *Genes Dev.*, 11: 2822-2834, 1997.
- Otsuka, T., Takayama, H., Sharp, R., Celli, G., LaRochelle, W. J., Bottaro, D. P., Ellmore, N., Vieira, W., Owens, J. W., Anver, M., and Merlino, G. c-Met autocrine activation induces development of malignant melanoma and acquisition of the metastatic phenotype. *Cancer Res.*, 58: 5157-5167, 1998.

20. Beermann, F., Hunziker, A., and Foletti, A. Transgenic mouse models for tumors of melanocytes and retinal pigment epithelium. *Pigm. Cell Res.*, *12*: 71–80, 1999.
21. Richmond, A., Lawson, D. H., Nixon, D. W., Stevens, J. S., and Chawla, R. K. Extraction of a melanoma growth-stimulatory activity from culture medium conditioned by the Hs294T human melanoma cell line. *Cancer Res.*, *43*: 2106–2112, 1983.
22. Richmond, A., Balentien, E., Thomas, H. G., Flaggs, G., Barton, D. E., Spiess, J., Bordoni, R., Francke, U., and Derynck, R. Molecular characterization and chromosomal mapping of melanoma growth stimulatory activity, a growth factor structurally related to β -thromboglobulin. *EMBO J.*, *7*: 2025–2033, 1988.
23. Anisowicz, A., Bardwell, L., and Sager, R. Constitutive overexpression of a growth regulated gene in transformed Chinese hamster and human cells. *Proc. Natl. Acad. Sci., USA*, *84*: 7188–7192, 1987.
24. Haskill, S., Peace, A., Morris, J., Sporn, S. A., Anisowicz, A., Lee, S. W., Smith, T., Martin, G., Ralph, P., and Sager, R. Identification of three related human GRO genes encoding cytokine functions. *Proc. Natl. Acad. Sci. USA*, *87*: 7732–7736, 1990.
25. Tekamp-Olson, P., Gallegos, C., Bauer, D., McClain, J., Sherry, B., Fabre, M., van Deventer, S., and Cerami, A. Cloning and characterization of cDNAs for murine macrophage inflammatory protein 2 and its human homologues. *J. Exp. Med.*, *172*: 911–919, 1990.
26. Dezube, B. J., Pardee, A. B., Beckett, L. A., Ahlers, C. M., Ecto, L., Allen-Ryan, J., Anisowicz, A., Sager, R., and Crumacker, C. S. Cytokine dysregulation in AIDS: *in vivo* overexpression of mRNA of tumor necrosis factor- α and its correlation with that of the inflammatory cytokine GRO. *J. Acquir. Immune Defic. Syndr.*, *5*: 1099–1104, 1992.
27. Rodeck, U., Melber, K., Kath, R., Menssen, H-D., Varello, M., Atkinson, B., and Herlyn, M. Constitutive expression of multiple growth factor genes by melanoma cells but not normal melanocytes. *J. Invest. Dermatol.*, *97*: 20–26, 1991.
28. Lazar-Molnar, E., Hegyesi, H., Toth, S., and Falus, A. Autocrine and paracrine regulation by cytokines and growth factors in melanoma. *Cytokine*, *12*: 547–554, 2000.
29. Wang, D., and Richmond, A. MGSA/GRO. In: J. J. Oppenheim (ed.), *On-Line Cytokine Book*, pp. 1023–1048. London, United Kingdom.
30. Balentien, E., Mufson, B. E., Shattuck, R. L., Derynck, R., and Richmond, A. Effects of MGSA/GRO α on melanocyte transformation. *Oncogene*, *6*: 1115–1124, 1991.
31. Owen, J. D., Strieter, R., Burdick, M., Haghnegahdar, H., Nanney, L., Shattuck-Brandt, R., and Richmond, A. Enhanced tumor-forming capacity for immortalized melanocytes expressing melanoma growth stimulatory activity/growth-regulated cytokine β and γ proteins. *Int. J. Cancer*, *73*: 94–103, 1997.
32. Haghnegahdar, H., Strieter, R., Burdick, M., Nanney, L. B., Cardwell, N., Shattuck-Brandt, R., and Richmond, A. MGSA/GRO production regulates melanoma tumor growth and angiogenesis. *J. Leukoc. Biol.*, *67*: 53–62, 2000.
33. Bordoni, R., Fine, R., Murray, D., and Richmond, A. Characterization of the role of melanoma growth stimulatory activity (MGSA) in the growth of normal melanocytes, nevocytes, and malignant melanocytes. *J. Cell. Biochem.*, *44*: 207–219, 1990.
34. Ganss, R., Montoliu, L., Monaghan, A. P., and Schutz, G. A cell-specific enhancer far upstream of the mouse tyrosinase gene confers high level and copy number-related expression in transgenic mice. *EMBO J.*, *13*: 3083–3093, 1994.
35. Serrano, M., Lee, H., Chin, L., Cordon-Cardo, C., Beach, D., and DePinho, R. A. Role of the INK4a/ARF locus in tumor suppression and cell mortality. *Cell*, *85*: 27–37, 1996.
36. Ruiz, A., Puig, S., Lynch, M., Castel, T., and Estivill, X. Retention of the CDKN2A locus and low frequency of point mutations in primary and metastatic cutaneous malignant melanoma. *Int. J. Cancer*, *76*: 312–316, 1998.
37. Krimperfort, P., Quon, K. C., Mooe, W. J., Loonstra, A., and Berns, A. Loss of p16^{Ink4a} confers susceptibility to metastatic melanoma in mice. *Nature (Lond.)*, *413*: 83–86, 2001.
38. Sharpless, N. E., Bardeesy, N., Lee, K-H., Carrasco, R., Castrillon, D. H., Aguirre, A. J., Wu, E., Horner, J. W., and DePinho, R. A. Loss of p16^{Ink4a} with retention of p19^{Arf} predisposes mice to tumorigenesis. *Nature (Lond.)*, *413*: 86–91, 2001.
39. Devalaraja, M. N., Wang, D. Z., Ballard, D. W., and Richmond, A. Elevated constitutive I κ B kinase activity and I κ B- α phosphorylation in Hs294T melanoma cells lead to increased basal MGSA/GRO- α transcription. *Cancer Res.*, *59*: 1372–1377, 1999.
40. Loukinova, E., Dong, G., Enamorado-Ayalya, I., Thomas, G. R., Chen, Z., Schreiber, H., and Van Waes, C. Growth regulated oncogene- α expression by murine squamous cell carcinoma promotes tumor growth, metastasis, leukocyte infiltration and angiogenesis by a host CXC receptor-2 dependent mechanism. *Oncogene*, *19*: 3477–3486, 2000.
41. Wang, H. Q., and Smart, R. C. Overexpression of protein kinase C- α in the epidermis of transgenic mice results in striking alterations in phorbol ester-induced inflammation and COS-2, MIP-2 and TNF- α expression but not tumor promotion. *J. Cell Sci.*, *112*: 3497–3506, 1999.
42. Faunce, D. E., Sonoda, K. H., and Stein-Streilein, J. MIP-2 recruits NKT cells to the spleen during tolerance induction. *J. Immunol.*, *166*: 313–321, 2001.
43. Singh, R. K., Gutman, M., Radinsky, R., Bucana, C. D., and Fidler, I. J. Expression of interleukin 8 correlates with the metastatic potential of human melanoma cells in nude mice. *Cancer Res.*, *54*: 3242–3247, 1994.
44. Schadendorf, D., Moller, A., Algermissen, B., Worm, M., Sticherling, M., and Czarnetzki, B. M. IL-8 produced by human malignant melanoma cells *in vitro* is an essential autocrine growth factor. *J. Immunol.*, *151*: 2667–2675, 1993.

Cancer Research

The Journal of Cancer Research (1916–1930) | The American Journal of Cancer (1931–1940)

Induction of Melanoma in Murine Macrophage Inflammatory Protein 2 Transgenic Mice Heterozygous for Inhibitor of Kinase/Alternate Reading Frame

Jinming Yang, Jing Luan, Yingchun Yu, et al.

Cancer Res 2001;61:8150-8157.

Updated version Access the most recent version of this article at:
<http://cancerres.aacrjournals.org/content/61/22/8150>

Cited articles This article cites 41 articles, 16 of which you can access for free at:
<http://cancerres.aacrjournals.org/content/61/22/8150.full#ref-list-1>

Citing articles This article has been cited by 6 HighWire-hosted articles. Access the articles at:
<http://cancerres.aacrjournals.org/content/61/22/8150.full#related-urls>

E-mail alerts [Sign up to receive free email-alerts](#) related to this article or journal.

Reprints and Subscriptions To order reprints of this article or to subscribe to the journal, contact the AACR Publications Department at pubs@aacr.org.

Permissions To request permission to re-use all or part of this article, use this link
<http://cancerres.aacrjournals.org/content/61/22/8150>.
Click on "Request Permissions" which will take you to the Copyright Clearance Center's (CCC) Rightslink site.